CHAPTER 6

A NOTE ON THE DEVELOPMENT OF WIND WAVES IN AN EXPERIMENT

Tokuichi Hamada, Akihiko Shibayama and Hajime Kato
Port & Harbour Research Institute, Japan

ABSTRACT

This is a note paper of experiment in an air-water experimental waterway. Two cases of the uniform depth of water 50 cm and of the uniform depth of water 15 cm are examined. The boundary condition for air flow is not changed. In a condition of almost the same discharge of air flow on the water surface, the development of wind waves is investigated. The properties of wind waves are slightly different in each case, but the analysis of physical mechanism of the development suggests that almost the same mechanism is active throughout both cases. Stillmore the portion of tangential stress, which is apparently transfered to wave momentum, is numerically obtained, and it is not so different in both cases of depth of water.

INTRODUCTION

We have already reported the experimental results of development of wind waves in the case of deep water (T. Hamada *et al.*(1963)), and the mechanism of wave development has been discussed using the similar analysis with the papers of J. W. Miles (1957, 1960). Because the actual distributions of the appeared non-negative damping factor in this case has not been so simple as those predicted by the linear theory, the accumulation of experimental data in various cases is desirable to obtain the reliable conclusions. This note, in which two different cases of depth of water are pursued, is concerned with the above-mentioned version.

In the case of depth of water 15 cm, the low frequency part of wind waves should be treated as the case of finite depth of water. The case of depth of water 50 cm, of course can be treated as in deep water. Properties of waves are summarized using the same method of adjustment, and their common features are analysed. The results clarify the fundamental characteristics of wind waves in the case when the velocity of wind is far greater than the celerity of generated waves.

EXPERIMENTS

The waterway used in this experiment is already explained (T. Hamada *et al.*(1963)). The length of its uniform part is 2850 cm, and this part is used for the measurement. Its width is 150 cm. The depth of water to the bottom is taken to 50 cm and 15 cm uniformly at each experiment. The height of air flow on the water surface is always 80 cm. The revolution number of air blower can be regulated, and is kept to r.p.m. 400 in the present cases. Therefore the maximum velocity at the middle of wind tunnel is almost same in each case. All measurements of wind and waves were executed at the precisely stationary states. The velocity of air flow was measured at B_a (965 cm leeward the section where the air flow initially touches the surface of water), C_a (1865 cm leeward the same section) and D_a (2765 cm leeward the same section). The properties of waves were measured at B_w, C_w and D_w each 10 cm leeward of B_a, C_a and D_a, respectively.

The velocity of air flow was measured by the method of pitot tube. The shearing stress of air flow on water surface (τ_0, $U_* = \sqrt{\tau_0/\rho}$) and the parameter z_0 are numerically computed by the logarithmic law of air flow using the measured wind velocity. Here we assumed that the water surface is completely rough, because the pertinent separation of viscous shear was not possible at the present state.

The velocity of the lowest layer of air flow cannot be accurately measured, because the water surface is covered by the succession of steep waves. Stillmore the direct application of logarithmic profile law to this lowest layer contains some doubt. Therefore we applied the logarithmic profile law to a little higher layer, and τ_0 and z_0 in this case may be a little greater than their appropriate values. Table - 1 (for the depth of water 50 cm) and Table - 2 (for the depth of water 15 cm) show the measured results. In both tables U_{40cm} is almost same, indicating that the discharge of air flow does not vary in both cases. But τ_0 and z_0 have some peculiar tendencies. They are generally smaller in the case of depth of water 15 cm. The corresponding values of γ^2_{1000cm} also show the same tendency.

Concerned to the property of waves, we made the frequency spectrum of surface wave profile by the analogue method of heterodyne detection (W. J. Pierson Jr. (1954)). χ^2- freedom of each obtained spectrum is adjusted to 36. In the case of depth of water 50 cm the average of three spectra at the stationary condition of each section is used. In the case of depth of water 15 cm the average of nine spectra, which are obtained equally at the middle and its both sides of each section, is used. By this way the intensity of spectrum considered in the following analysis is considered sufficiently reliable. The main characteristics of averaged spectrum are shown in Table - 3 (for the depth of water 50 cm) and in Table - 4 (for the depth of water 15 cm). The effect of weak drift current, which appears at the case of water depth 15 cm, is neglected.

The remarkable point is that the increase rate of $\overline{\eta^2}$ of both cases is different, and the increase of $\overline{\eta^2}$ and of $\overline{H}_{1/3}$ along the fetch distance is relatively small in the case of water depth 15 cm. $\bar{f}_{\text{zero up-cross}}$ is a little larger in the case of depth of water 15 cm. As the influence of weak drift current is not explicit, the meaning of this increase is not conclusive. ε , which is the parameter for the band width of spectrum, is not so different in both cases.

Averaged frequency spectra at B_w, C_w and D_w are shown in Fig - 1 (for the depth of water 50 cm) and in Fig - 2 (for the depth of water 15 cm). The general tendency is in good agreement at both cases. The slope of high frequency part is very steep, and the value of n at the expression $E(f) \sim f^{-n}$ is shown in Table - 3 and in Table - 4. It is far greater than 5.

ANALYSIS

The analysis of experimental data accords with following three aspects of physical process. They are (i) the determination of non-negative damping factor numerically computed from wind and wave data, (ii) the determination of the portion of tangential surface stress of wind, which is apparently transfered to the momentum of waves, and (iii) the determination of the ratio of the attenuation of high frequency part of the spectrum in the case where n is sufficiently greater than 5 at the expression $E(f) \sim f^{-n}$.

(I) In the present treatment we consider that the development of wind waves is mainly controlled by the mechamism suggested by H. Jeffreys (1925, 1926) and J. W. Miles (1957, 1960). The brief explanation of the mathematical treatment was already reported in the case of deep water (T. Hamada (1963)). In the case of the finite depth of water, the following relations are obtained in the two-dimensional treatment.

$$E(\omega) = \int_{-\frac{\pi}{2}}^{\frac{\pi}{2}} \exp\left\{ -k^2\sqrt{\frac{\nu}{2kC_0}} \frac{2\,Fe \sec\alpha}{\sinh kh \cosh kh + kh} - \frac{8\nu k^2}{C_0} \frac{Fe \sec\alpha}{1 + \frac{kh}{\sinh kh \cosh kh}} \right.$$

$$\left. + \frac{2s}{g} U_1^2 \cos\alpha \cdot k^2 \left(m'_{12}(K) + n'_{11}(K) \coth kh \right) \frac{Fe}{1 + \frac{kh}{\sinh kh \cosh kh}} \right\} \times 4\phi(\omega,\alpha)_{Fe=0}$$

$$\times \frac{k\omega}{g \tanh kh + khg \,\mathrm{sech}^2 kh}\, d\alpha \qquad (1)$$

$$E(\omega)_{Fe=0} = \int_{-\frac{\pi}{2}}^{\frac{\pi}{2}} 4\phi(\omega,\alpha)_{Fe=0} \frac{k\omega}{g \tanh kh + khg\, \mathrm{sech}^2 kh}\, d\alpha \qquad (2)$$

$$C_0 = \left\{ \frac{g + T'k^2}{k} \tanh kh \right\}^{\frac{1}{2}}, \quad U_1 = \frac{U_*}{K} \ (K \simeq 0.4), \quad \omega = 2\pi f \qquad (3)$$

In the above relations we used

$$C_g \simeq \frac{C_0}{2}\left(1 + \frac{kh}{\sinh kh \cosh kh} \right)$$

as the velocity of the energy transmission of wave. Strictly

$$C_g = \frac{C_0}{2}\left(1 + \frac{kh}{\sinh kh \cosh kh} \right) + \frac{C_0 T' k^2}{g + T'k^2}$$

should be used. But the difference is quite negligible in the present case. The relation (1) indicates the change of spectrum intensity caused by both the viscous effect and the amplification mechanism from wind. The first term in exponent means the viscous attenuation by bottom friction. The second term means the viscous attenuation by internal friction, and this effect concentrates near water surface. The third term indicates the amplification mechanism. The expression is given in the same way of J. W. Miles (1957), $m'_{12}(K)$ is the non-nagative damping factor by the normal stress of air flow, and therefore it has the same meaning with β of J. W. Miles. $n'_{11}(K) \coth kh$ is due to the oscillatory tangential stress of air flow, and is considered to be far smaller than $m'_{12}(K)$ in general.

(In this paper we simply put $m'_{12}(K) + n'_{11}(K)\coth kh \simeq m'_{12}(k) + n'_{11}(k)\coth kh$.)

The above relations are strictly deduced from the linear theory of wave development, but actually the experimental data contain more complicated factors. Especially, in the high frequency part of the spectrum, the relation (1) is not pertinent to explain the change of the spectrum intensity. In this experiment $m'_{12}(k) + n'_{11}(k)\coth kh$ becomes negative in the above-mentioned region, and this means that the non-negative damping factor from wind is replaced by the more influential attenuation factor, which does not appear in the linear relation (1). Accordingly we should consider that negative $m'_{12} + n'_{11}\coth kh$ in this case is a converted value from the actual mechanism of the attenuation.

In the ralations (1) and (2) we should assume the directional spreading of waves. The used assumption is that in the case of depth of water 50 cm the directional spreading can be neglected, and that in the case of depth of water 15 cm the directional spectrum has the same intensity in $|\alpha| \leq 50°$ and otherwise zero. But a treatment of no directional spreading is also used for the comparison in the case of depth of water 15 cm.

The results of numerical computations are shown in Fig - 3, - 4 (for the depth of water 50 cm) and in Fig - 5, - 6 (for the depth of water 15 cm). In these figures the distribution of $m'_{12}(k) + n'_{11}(k)\coth kh$ around the peak of the spectrum is in good agreement for the case of the same distance from the air inlet in spite of the change of the depth of water. At the low frequency part obtained values of $m'_{12}(k) + n'_{11}(k)\coth kh$ are the same order as the computed values of J. W. Miles (1960), but the distribution is quite different. In every case the value of $m'_{12}(k) + n'_{11}(k)\coth kh$ gradually decreases in that region from the lowest frequency to the peak of spectrum, and at the high frequency part it always becomes negative. At the highest frequency it approaches to zero. By this way we have obtained the similar value and the similar distribution of $m'_{12}(k) + n'_{11}(k)\coth kh$ through both cases of depth of water. This shows that almost the same mechanism of wave development is active in both cases. The analysis of distribution of $m'_{12}(k) + n'_{11}(k)\coth kh$ seems to be one of the future problem.

(II) The contribution τ_{OW} means originally the portion of τ_O, which is transfered to wave momentum through the interaction of water surface. τ_{OW} may be computed by

$$\tau_{ow} = \rho_a U_1^2 \int_0^\infty \int_{-\frac{\pi}{2}}^{\frac{\pi}{2}} m'_{12}(k) \cos^2\alpha \, k^2 S(k,\alpha)\, k \, dk \, d\alpha \tag{4}$$

$$\overline{\eta^2} = \int \frac{S(K)}{2} dK = \int_0^\infty \int_{-\frac{\pi}{2}}^{\frac{\pi}{2}} S(k,\alpha)\, k \, dk \, d\alpha \tag{5}$$

Because $n'_{11}(k)\coth kh$ seems far smaller than $m'_{12}(k)$, we use $m'_{12}(k) + n'_{11}(k)\coth kh$ given by (1) for $m'_{12}(k)$ in (4). There is still a fundamental problem that, at the high frequency part, the appeared non-negative damping factor is negative, and does not indicate the true meaning of physical process. Accordingly the true value of τ_{OW} in the present experiment cannot be measured in anyway. But, if we apply the relation (4) to the low frequency part from the peak of the spectrum (where $m'_{12}(k) + n'_{11}(k)\coth kh$ is positive and its value seems appropriate), the computed result will show the increase of the actual momentum of progressive waves in the concerned part of the spectrum, and it will be approximately attributed to the action of normal stress from wind.

τ_{ow} for the low frequency part of the spectrum is thus obtained. Table - 5 shows the result. The ratio τ_{ow}/τ_o and $\tau_{ow}/0.8\ \tau_o$ are given in it. It may be probable that the true value of τ_{ow}/τ_o situates between these two values. Generally speaking it lies between 0.15 and 0.20, and is a little smaller in the case of depth of water 15 cm.

The above-mentioned method of deduction is very different from the paper of R. W. Stewart (1961), which is concerned with the wind wave in actual ocean. Nevertheless the result seems comparable. As the method is not found to estimate the true $m_{12}'(k)$ at the high frequency part, the true value of τ_{ow}/τ_o cannot be accurately pursued at the present situation. (At the high frequency part of the spectrum very small $m_{12}'(k)\ (>0)$ seems effective to increase τ_{ow}.)

(III) The rapid attenuation of the high frequency part of spectrum, which occurs with the increase of the travelling distance of wave, is perceived in Fig - 1 and Fig - 2. On the other hand T. Hamada (1964) has already shown that the rapid attenuation of the same part of the spectrum of wind-generated waves may be possible even at the calm air condition, if n is greater than 5 at the expression $E(f) \sim f^{-n}$. The discussion in the above-mentioned paper has been in a condition that the breaking of waves did not appear and the generation of surface capillary waves was very weak. In the present case waves are directly influenced by air flow, and the breaking of wave surface and the generation of surface capillary waves are explicitly noticed. By this way the physical condition of water surface is very different in these two cases. But the value of n at $E(f) \sim f^{-n}$ in each case situates between 7 and 10, and it is sufficiently greater than 5. To clear up the condition of the attenuation, the rate of attenuation of the spectrum intensity at the depth of water 15 cm is examined in connection with the travelling distance of wave energy. We use the spectra of Fig - 2 of this paper and Fig - 4, - 5 of the previous paper (T. Hamada (1964)).

The following coefficient is used. Its application is of course confined within the high frequency part which attenuates with the progress of waves.

$$\frac{E(f)_{(1)} - E(f)_{(2)}}{E(f)_{(2)} \cdot x} \tag{6}$$

x means the direct distance of two stations for measurement, and the effect of the angular spreading is neglected. Putting $E(f)_{(0)}$ as $E(f)$ at $x = 0$, $E(f)_{(1)}$ means the actually attenuated spectrum at $x = x$. $E(f)_{(2)}$ is for the assumed spectrum attenuated by molecular viscosity only. Accordingly,

$$\left.\begin{aligned} E(f)_{(1)} &= E(f)_{(0)}\, e^{-\alpha_1(\nu)x - \alpha_2 x} \\ E(f)_{(2)} &= E(f)_{(0)}\, e^{-\alpha_1(\nu)x} \end{aligned}\right\} \tag{7}$$

and so,

$$\frac{E(f)_{(1)} - E(f)_{(2)}}{E(f)_{(2)} \cdot x} \fallingdotseq -\alpha_2 \tag{8}$$

Therefore this coefficient means the attenuation rate caused by physical effect except the molecular viscosity. The numerical results are shown in Fig - 7. In this figure the maximum of the absolute value of the coefficient (6) has similar values in both case of direct wind effect and of no wind effect. The value is $7 \times 10^{-4} \sim 10 \times 10^{-4}$ in cm^{-1}. The form of distribution of the coefficient (6) in concern with the frequency f is also similar in both cases. As the effect of angular spreading of waves is not so large, this result can be reliable in connection with the travelling distance of wave energy.

The result suggests us to consider that this attenuation of the high frequency part of the spectrum is primarily correlated with the slope of the spectrum at the concerned part. The instability of wave surface and the generation of capillary waves are not the main controlling factors on this part of the spectrum. Stillmore the strong influence of the non-negative damping factor seems doubtful in this part of the spectrum, though it is a main controlling factor on the low frequency part. (The tertiary and higher order interactions for the energy transport in different two-dimensional frequency components of waves do not seem to have strict experimental verification in the present stage, and so it contains some uncertainty in its amounts.)

CONCLUSIONS

(I) In this experiment the distribution of non-negative damping factor $m'_{12}(k) + n'_{11}(k) \coth kh$ shows very similar tendencies and values in both cases of depth of water 50 cm and 15 cm, and at the low frequency part its values are comparable to those obtained by J. W. Miles (1960) theoretically. This result means that almost the same mechanism of wave development is active in both cases of deep water and of relatively shallow water. But the distribution of $m'_{12}(k) + n'_{11}(k) \coth kh$ indicates that in every case the values are controlled by the form of the spectrum. Because this is not explained by the instability theory of J. W. Miles (1960), some comprehensive theory seems necessary to clarify this phenomenon.

(II) The appeared non-negative damping factor is always negative in the high frequency part of wave spectra, and the energy of this part of spectra attenuates. In this experiment n is about 10 at the expression of spectrum $E(f) \sim f^{-n}$, and the rapid attenuation is expective at this part of spectrum. At the same time the actual (positive) non-negative damping factor given by wind seems very small in the high frequency region of the spectrum.

(III) The portion of the shearing stress τ_{0W}, which gives actually the wave momentum at the low frequency part of wave spectra, amounts to about 20 % of the total shearing stress τ_0, which is determined by the velocity profile of air flow. The contribution from the high frequency part of the spectrum cannot be determined in the present experiment. The above-mentioned ratio becomes a little smaller at the case of the depth of water 15 cm, and it is comparable to the value estimated by R. W. Stewart (1961), who used the observed data in actual ocean.

(IV) In the case of depth of water 15 cm the rate of attenuation of the high frequency part of the spectrum in connection with the travelling distance of wave energy has almost similar tendencies in both cases of wind-generated waves at the calm condition and of wind waves at the direct wind action. (In these cases n is $7.7 \sim 11.1$ at $E(f) \sim f^{-n}$.) The maximum value of this rate in each case concentrates to $7 \times 10^{-4} \sim 10 \times 10^{-4}$ in cm^{-1}.

This means that the same mechanism of attenuation (T. Hamada (1964)) is active in both cases, and it seems that the supply of energy from wind to this part of the wave spectrum, the breaking of wave surface and the generation of surface capillary waves are relatively weak factors for the control of high frequency part of the spectrum.

The authors are grateful to members of our laboratory for their helps in experiment and in numerical computations.

References

Hamada, T. *et al.* (1963) An experimental study of development of wind waves. Report No. 2, Port & Harbour Research Institute, Japan

Hamada, T. (1964) On the f^{-5} law of wind-generated waves. Report No. 6 Port & Harbour Research Institute, Japan

Jeffreys, H. (1925) On the formation of water waves by wind, Proc. Roy. Soc. A. Vol. 107.

Jeffreys, H. (1926) On the formation of water waves by wind (second paper), Proc. Roy. Soc. A. Vol. 110.

Miles, J. W. (1957) On the generation of surface waves by shear flows, J. Fluid Mech. Vol. 3.

Miles, J. W. (1960) On the generation of surface waves by turbulent shear flows, J. Fluid Mech. Vol. 7.

Pierson Jr. W. J. (1954) An electronic wave spectrum analyzer and its use in engineering problems, B. E. B. Tech. Memo., No. 56.

Stewart, R. W. (1961) The wave drag of wind over water, J. Fluid Mech. Vol. 10

Table 1. Characteristics of Wind

depth of water 50 cm , r.p.m. 400 (ρ_a = 0.00122 ~ 0.00123)

Station		τ_0 dyne/cm^2	U_* cm/sec	Z_0 cm	U_{1000} cm/sec	U_{40} cm/sec	$Z_0/H_{1/3}$	$H_{1/3}$	γ^2_{1000}
B_a		11.13	95.53	0.179	2076	1168	0.0440	4.01	2.11×10^{-3}
C_a		12.66	101.3	0.248	2115	1284	0.0397	6.24	2.29×10^{-3}
D_a	L = 35	9.65	89.45	0.104	2046	1250			1.91×10^{-3}
	75	12.84	103.35	0.182	2218	1367	0.0236	7.70	2.17×10^{-3}
	115	12.07	100.18	0.200	2162	1292			2.14×10^{-3}

Table 2. Characteristics of Wind

depth of water 15 cm , r.p.m. 400 (ρ_a = 0.00117 ~ 0.00118)

Station		τ_0 dyne/cm^2	U_* cm/sec	Z_0 cm	U_{1000} cm/sec	U_{40} cm/sec	$Z_0/H_{1/3}$	$H_{1/3}$	γ^2_{1000}
B_a	L=35	10.87	96.0	0.22	2010	1195			2.28×10^{-3}
	75	11.76	100.2	0.24	2080	1199	0.0432	4.32	2.31×10^{-3}
	115	8.82	87.0	0.10	2000	908			1.89×10^{-3}
C_a	L=35	9.13	88.0	0.22	1853	1156			2.25×10^{-3}
	75	8.18	83.3	0.13	1860	1219	0.0251	5.77	2.00×10^{-3}
	115	7.76	81.0	0.087	1895	1215			1.82×10^{-3}
D_a	L=35	6.60	75.0	0.047	1870	1229			1.60×10^{-3}
	75	7.56	80.4	0.074	1907	1296	0.0072	6.37	1.77×10^{-3}
	115	5.13	66.3	0.017	1815	1238			1.33×10^{-3}

Table 3. Characteristics of Waves

depth of water 50 cm , r.p.m. 400

Station	$\overline{\eta^2}$ cm^2	$H_{1/3}$ cm	$\overline{f}$ zero up-cross	$\overline{f}$ Max	f peak of spectrum	ε	$\frac{f \text{ paek of spectrum}}{\overline{f} \text{ zero up-cross}}$	$H_{1/3}/\overline{L}$ zero up-cross	n $dE(f) \sim f^{-n}$
B_w	1.00	4.01	2.58	3.12	2.30	0.562	0.891	$\frac{1}{5.85}$	10.0
C_w	2.43	6.24	1.95	2.27	1.85	0.512	0.948	$\frac{1}{6.57}$	13.1
D_w	3.71	7.70	1.71	2.26	1.55	0.653	0.906	$\frac{1}{6.93}$	10.9

Table 4. Characteristics of Waves

depth of water 15 cm , r.p.m. 400

Station	$\overline{\eta^2}$ cm²	$H_{1/3}$ cm	$\bar{f}$ zero up-cross	$\bar{f}_{Max}$	f peak of spectrum	ε	$\frac{f \text{ peak of spectrum}}{\bar{f} \text{ zero up-cross}}$	$H_{1/3}/L$ zero up-cross	h/L zero up-cross	n at $E(f) \sim f^{-n}$
B_w	1.17	4.32	2.72	3.19	2.45	0.521	0.90	$\frac{1}{4.86}$	$\frac{1}{1.41}$	10.8
C_w	2.09	5.77	2.12	2.40	1.95	0.464	0.92	$\frac{1}{5.80}$	$\frac{1}{2.29}$	10.0
D_w	2.55	6.37	1.84	2.16	1.65	0.525	0.90	$\frac{1}{7.04}$	$\frac{1}{2.98}$	7.7

Table 5. τ_{ow}/τ_o

Depth of water	situation	τ_o dyne/cm^2	τ_{ow} dyne/cm^2	τ_{ow}/τ_o	$\tau_{ow}/0.8\tau_o$
50 cm	B — C	11.9	1.85	0.156	0.195
50 cm	C — D	12.1	1.93	0.159	0.199
15 cm	B — C	9.42	1.31	0.139	0.174
15 cm	C — D	7.39	1.09	0.148	0.185

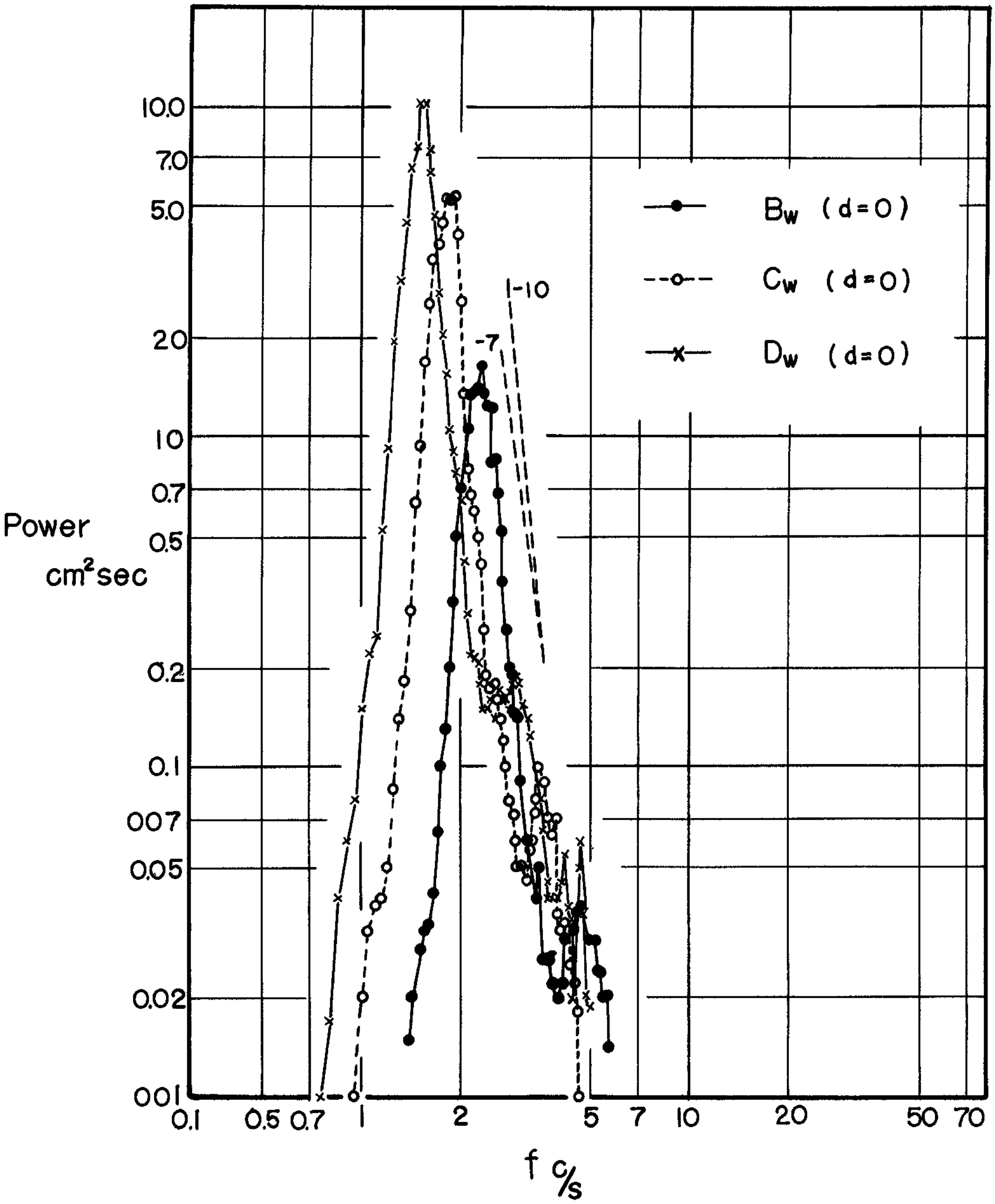

Fig. 1. Spectra of Wave Profile
depth of water 50 cm, r.p.m. 400

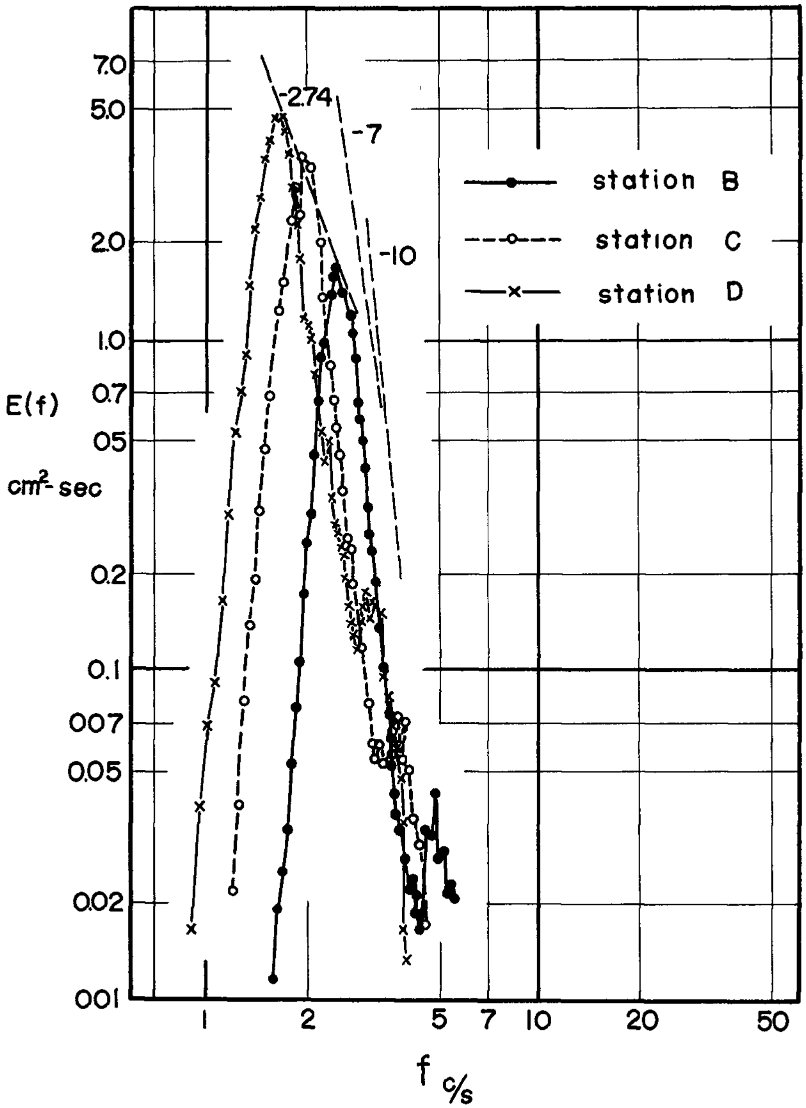

Fig. 2. Spectra of Wave Profile
depth of water 15 cm, r.p.m. 400

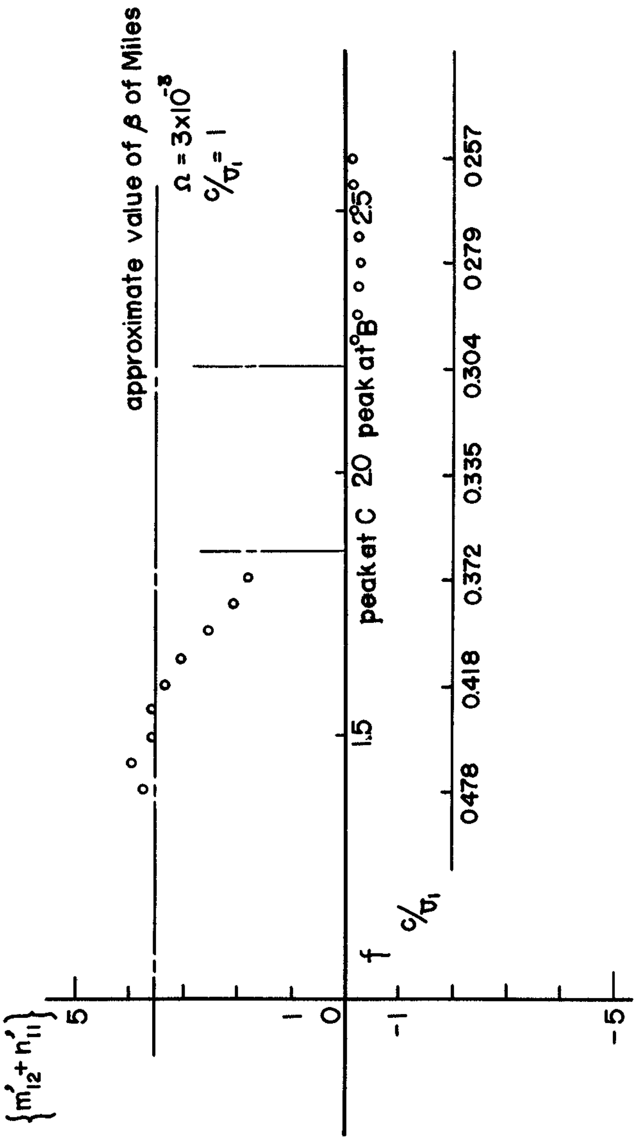

Fig. 3. Values of $(m'_{12} + n'_{11})$
Fetch between B_W and C_W
depth of water 50 cm, r.p.m. 400

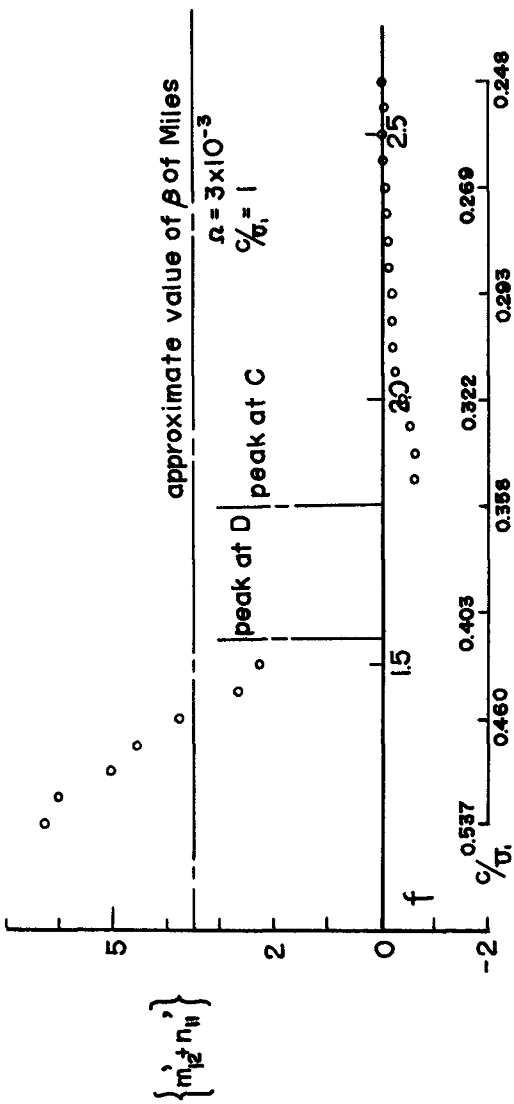

Fig. 4. Values of $(m'_{12} + n'_{11})$
Fetch between C_W and D_W
depth of water 50 cm, r.p.m. 400

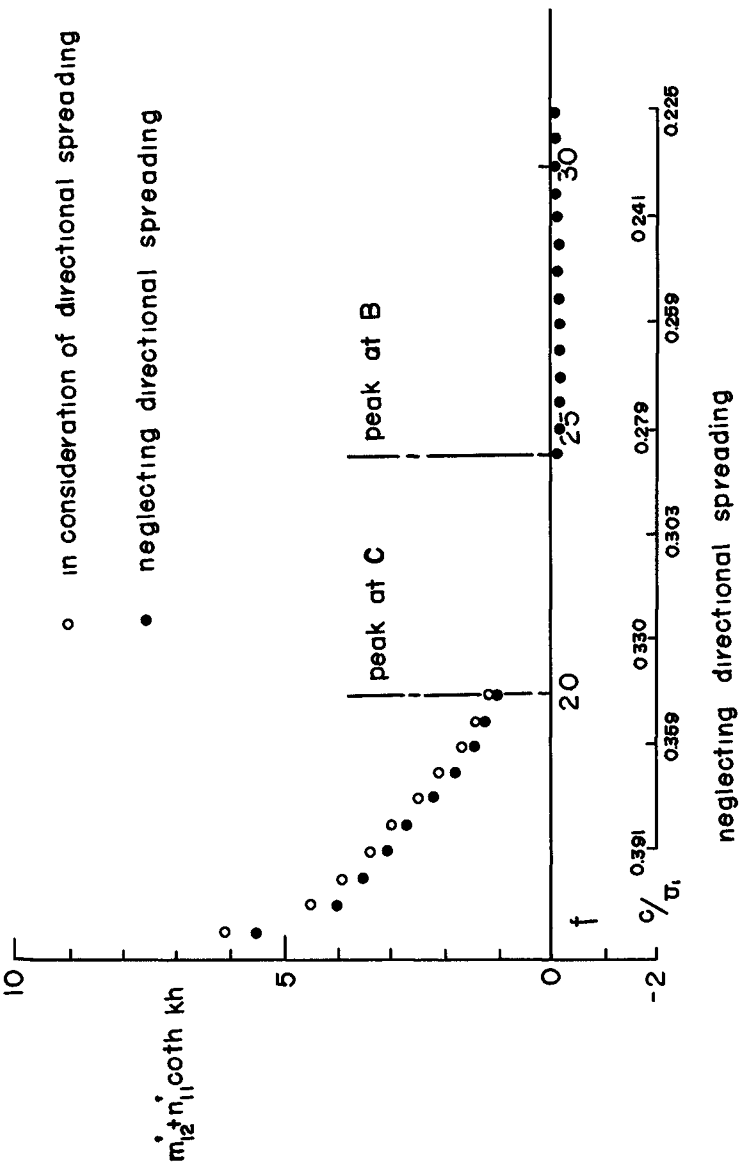

Fig. 5. Values of $(m'_{12} + n'_{11} \coth kh)$
Fetch between B_W and C_W
depth of water 15 cm, r.p.m. 400

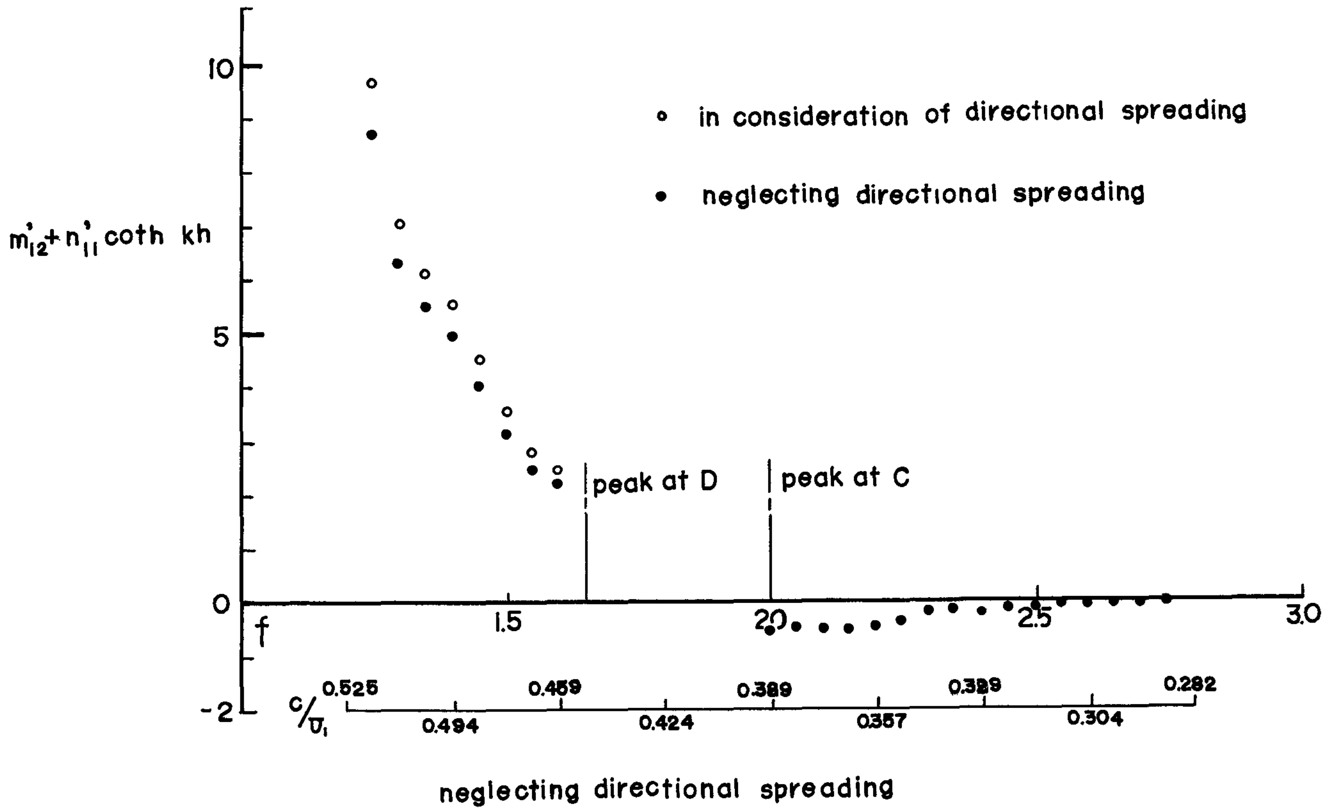

Fig. 6. Values of $(m'_{12} + n'_{11} \coth kh)$
Fetch between C_W and D_W
depth of water 15 cm, r.p.m. 400

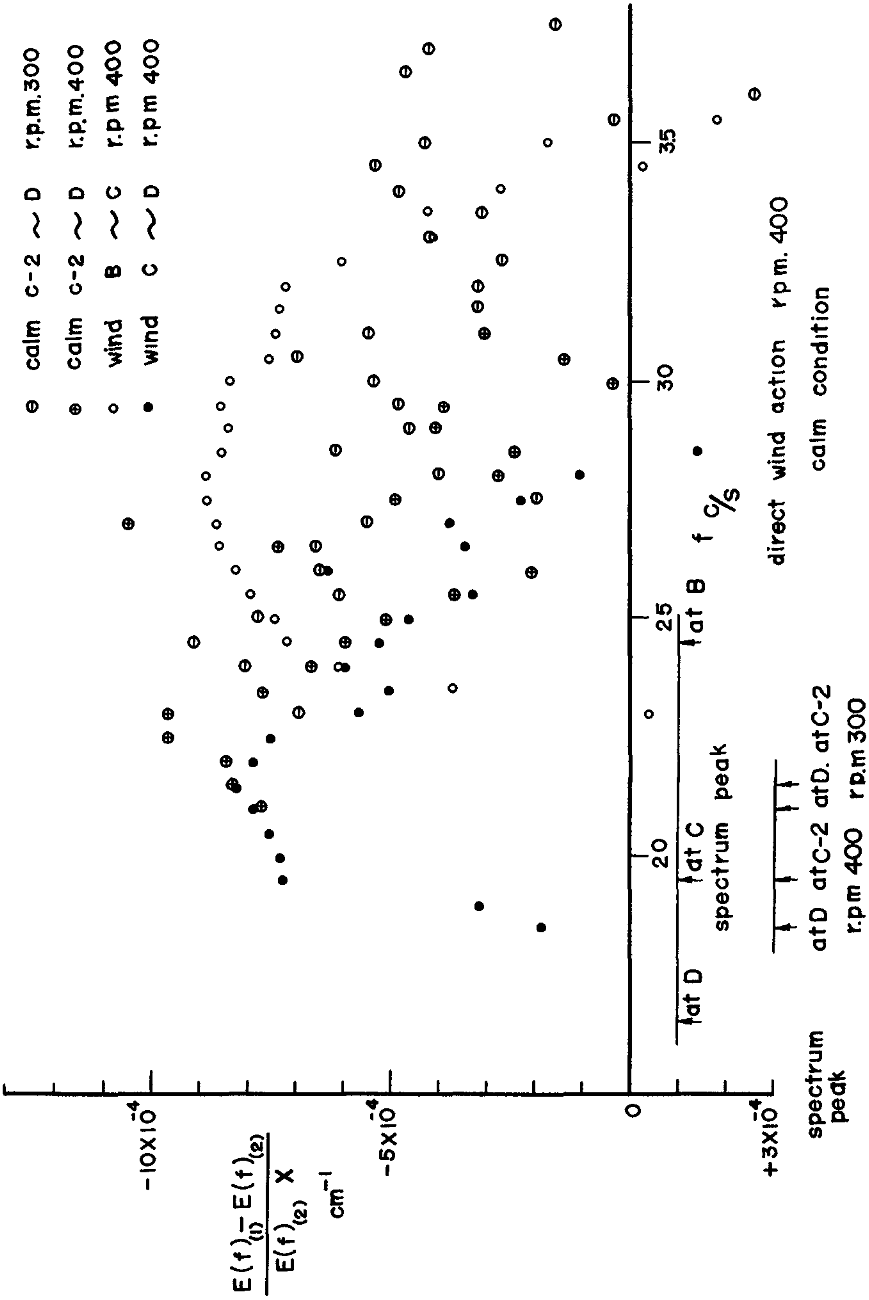

Fig. 7. Distribution of Attenuation Coefficient $\frac{E(f)_{(1)} - E(f)_{(2)}}{E(f)_{(2)} \cdot x}$